

AD-761 828

BARIUM CLOUD GROWTH AND STRIATION IN A
CONDUCTING BACKGROUND

Jeng-Nan Shiau, et al

Rochester University

Prepared for .

Rome Air Development Center
Advanced Research Projects Agency

November 1972

DISTRIBUTED BY:

NTIS

**National Technical Information Service
U. S. DEPARTMENT OF COMMERCE
5285 Port Royal Road, Springfield Va. 22151**

RADC-TR-72-320
Final Technical Report
November 1972



**BARIUM CLOUD GROWTH AND STRIATION
IN A CONDUCTING BACKGROUND**

University of Rochester

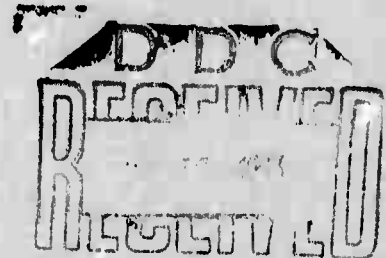
**Sponsored by
Defense Advanced Research Projects Agency
ARPA Order No. 1057**

**Approved for public release;
distribution unlimited.**

The views and conclusions contained in this document are those of the authors and should not be interpreted as necessarily representing the official policies, either expressed or implied, of the Defense Advanced Research Projects Agency or the U. S. Government.

NATIONAL TECHNICAL
INFORMATION SERVICE

**Rome Air Development Center
Air Force Systems Command
Griffiss Air Force Base, New York**



AD 761828

DOCUMENT CONTROL DATA - R & D

(Security classification of title, body of abstract and indexing annotation must be entered when the overall report is classified)

1. ORIGINATING ACTIVITY (Corporate author) University of Rochester River Campus Rochester, New York 14627		2a. REPORT SECURITY CLASSIFICATION Unclassified	
		2b. GROUP	
3. REPORT TITLE BARIUM CLOUD GROWTH AND STRIATION IN A CONDUCTING BACKGROUND			
4. DESCRIPTIVE NOTES (Type of report and inclusive dates) Final Technical Report 15 March 1972 - 15 November 1972			
5. AUTHOR(S) (First name, middle initial, last name) Jeng-Nan Shiau Albert Simon			
6. REPORT DATE November 1972	7a. TOTAL NO. OF PAGES 34 41	7b. NO. OF REFS 7	
8a. CONTRACT OR GRANT NO. F-30602-70-C-0001	9a. ORIGINATOR'S REPORT NUMBER(S)		
b. PROJECT NO. 10570202	9b. OTHER REPORT NO(S) (Any other numbers that may be assigned this report)		
c. Program Code Number: 2E20	RADC-TR-72-320		
d. ARPA Order Number: 1057			
10. DISTRIBUTION STATEMENT approved for public release; distribution unlimited			
11. SUPPLEMENTARY NOTES Monitored by Leonard Strauss RADC (OCSE) GAFB, N. Y. 13441 315-330-3451		12. SPONSORING MILITARY ACTIVITY Defense Advanced Research Projects Agency 1400 Wilson Blvd. Arlington, Va. 22209	
13. ABSTRACT Previous calculations of barium cloud growth failed to give reasonable estimates of striation scale size and onset time because they either assumed no ionospheric end-shortening or no ion diffusion (all modes unstable) or strong shortening (all modes stable). We derive a set of equations which include finite end-shortening and solve by a new numerical technique. For moderate end-shortening (in the experimental range) we obtain a fastest growing mode of reasonable size on the rear of the cloud. The growth rates and instability range are very sensitive to the end-shortening and magnitude of the ambient electric field. There is no growth below a critical value of E or above a critical value of the shortening. A series of graphs are presented. We also derive most previous results as special cases of our equations.			

1a

KEY WORDS

LINK A

LINK B

LINK C

ROLE

WT

ROLE

WT

ROLE

WT

- 1. Striations
- 2. ExB Instability
- 3. Cross Field Instability
- 4. Gradient Drift Instability
- 5. Barium Clouds

**BARIUM CLOUD GROWTH AND STRIATION
IN A CONDUCTING BACKGROUND**

**J. N. Shiau
A. Simon**

**Contractor: University of Rochester
Contract Number: F30602-70-C-0001
Effective Date of Contract: 14 September 1969
Contract Expiration Date: 31 December 1972
Amount of Contract: \$105,063.00
Program Code Number: 2E20**

**Principal Investigator: Prof. A. Simon
Phone: 716 275-4073**

**Project Engineer: Vincent J. Coyne
Phone: 315 330-3107**

**Contract Engineer: Leonard Strauss
Phone: 315 330-3451**

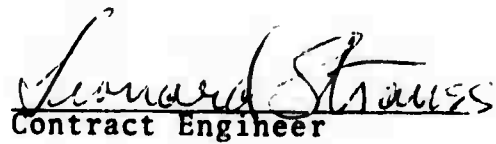
**Approved for public release;
distribution unlimited.**

**This research was supported by the
Defense Advanced Research Projects
Agency of the Department of Defense
and was monitored by Leonard Strauss
RADC (OCSE), GAFB, NY 13441 under
Contract F30602-70-C-0001.**

PUBLICATION REVIEW

This technical report has been reviewed and is approved


RADC Project Engineer


Contract Engineer

ABSTRACT

Previous calculations of barium cloud growth failed to give reasonable estimates of striation scale size and onset time because they either assumed no ionospheric end-shortening or no ion diffusion (all modes unstable) or strong shortening (all modes stable). We derive a set of equations which include finite end-shortening and solve by a new numerical technique. For moderate end-shortening (in the experimental range) we obtain a fastest growing mode of reasonable size on the rear of the cloud. The growth rates and instability range are very sensitive to the end-shortening and magnitude of the ambient electric field. There is no growth below a critical value of E or above a critical value of the shortening. A series of graphs are presented. We also derive most previous results as special cases of our equations.

TABLE OF CONTENTS

	<u>Page</u>
Abstract.	iii
List of Illustrations	vii
Introduction.	1
Basic Equations	2
Dynamical Equations for Equilibrium and Perturbations	7
Numerical Solutions and Discussion.	11
Appendix A: Special Cases Yielding Previous Results	17
Appendix B: Computational Procedure.	21
Acknowledgment.	22
References.	22

LIST OF ILLUSTRATIONS

- Fig. 1 Equilibrium growth for shorting ratios $\lambda=0.25$, 4 and 50.
- Fig. 2 Time evolution of r.m.s. density perturbation for various k^* ($\Omega\tau=10$, $\lambda=4$, $E_x^*=1$, $E_y^*=-10$).
- Fig. 3 Growth of $k^*=4$ perturbation in x-space and time ($\Omega\tau=10$, $\lambda=4$, $E_x^*=1$, $E_y^*=-10$).
- Fig. 4 Growth rate γ (at $t^*=0.02$) versus k^* for various shorting ratios λ ($\Omega\tau=10$, $E_x^*=1$, $E_y^*=-10$).
- Fig. 5 Growth rate γ (at $t^*=0.2$) versus k^* for various magnitudes of the ambient electric field ($\Omega\tau=10$, $\lambda=4$, $E_y^*/E_x^*=10$).
- Fig. 6 Maximum growth rate γ_{MAX} (at $t^*=0.2$) as a function of E_y^* for various values of γ ($\Omega\tau=10$, $E_y^*/E_x^*=-10$).
- Fig. 7 Growth rate γ (at $t^*=0.2$) versus k^* for various angles between E_A and the x-direction ($\Omega\tau=10$, $\lambda=4$, $|E_A|=(301)^{1/2}$).
- Fig. 8 Growth rate γ (at $t^*=0.2$) versus k^* for various angles between E_A and the x-direction and for $|E_A|=5.0$ and 3.0 respectively ($\Omega\tau=10$, $\lambda=4$).
- Fig. 9 Growth rate γ (at $t^*=0.02$) versus k^* for various values of $\Omega\tau$ ($\lambda=4$, $E_x^*=1$, $E_y^*=-10$).
- Fig. 10 Maximum growth rate γ_{MAX} times $\Omega/[1+(\Omega\tau)^2]$ as a function of $(\Omega\tau)$ ($\lambda=4$, $E_y^*=1$, $E_x^*=-10$).
- Fig. 11 Perturbed density contours for the $k^*=4$ mode at $t^*=0.2$ ($\Omega\tau=10$, $\lambda=4$, $E_x^*=1$, $E_y^*=-10$).
- Fig. 12 Perturbed potential (ϕ_1) contours for the $k^*=4$ mode at $t^*=0.2$ ($\Omega\tau=10$, $\lambda=4$, $E_x^*=1$, $E_y^*=-10$).

There seems to be general agreement that the EXR instability [Simon, 1963] (sometimes called the gradient drift instability) is responsible for the onset of striations in barium clouds released in the ionosphere. However, the problem has been to demonstrate that this is actually so by calculating the scale size and delay time and making comparison with experiments. Previous attempts failed because they either predict instability for all wavelengths and with comparable growth rate [Linson and Workman, 1970; Völk and Haerendel, 1971] or because they predict stable behavior [Simon, 1970].

We have previously derived a set of equations [Simon and Sleeper, 1972] which govern the growth of a barium cloud immersed in a conducting medium. We now show that all earlier results are included as special cases of these equations corresponding to no end shorting or strong shorting or neglect of diffusion. In each of these cases, one can account for the results obtained. We have now perfected a new numerical scheme for solving these equations with arbitrary end-shortening. We find that there is a preferred wave number and growth rate and that the results are very sensitive to the amount of end shorting and to the strength of the external ambient electric field. For values comparable to those in actual releases, we find a growth rate and scale size in general agreement with the observations.

In the next section, we rederive the general equations from a slightly more general viewpoint. Following that we describe a particular solution of these equations. The

corresponding numerical solutions and a discussion of the results are then given. Finally, in Appendix A, we show that previous results are indeed special cases of our set of equations, while Appendix B gives details of the computational procedure.

BASIC EQUATIONS

We shall denote the number density of barium ions, ambient ions and electrons, respectively, by n_B , n_A and n_e . Each obeys the continuity equation

$$\frac{\partial n}{\partial t} + \nabla \cdot (n \underline{v}) = 0 \quad (1)$$

and quasineutrality holds, i.e.

$$|n_B + n_A - n_e| \ll n_e \quad (2)$$

where we assume singly charged ions, for simplicity. Denoting electrical current density per species as $J_B = e n_B v_B$, $J_A = e n_A v_A$, $J_e = -e n_e v_e$ and using Eqs. (1) and (2), one has

$$\nabla \cdot (\underline{J}_A + \underline{J}_B + \underline{J}_e) = 0 \quad (3)$$

and this equation can be used in place of the electron continuity equation.

The velocities are given by the usual diffusion relations in a magnetized medium

$$n v_{||} = -D \nabla_{||} n \pm \mu n E_{||} \quad (4)$$

$$n \underline{v}_{\perp} = [-D \nabla_{\perp} n \pm \mu_{\perp} n \underline{E}_{\perp}] \mp (\omega \tau) \underline{b} \times [-D \nabla_{\perp} n \pm \mu_{\perp} n \underline{E}_{\perp}] \quad (5)$$

written in the rest frame of the neutral background. The upper signs refer to ions and the lower to electrons and all symbols have their usual meaning in the neutral rest frame. The corresponding species current divergence is

$$\frac{1}{e} \nabla \cdot \underline{J} = \pm \nabla_{||} [-D \nabla_{||} n \pm \mu n E_{||}] \pm \nabla_{\perp} [-D_{\perp} \nabla_{\perp} n \pm \mu_{\perp} n \underline{E}_{\perp}] \pm \mu_{\perp} (\Omega \tau) \nabla n \times \underline{E}_{\perp} \cdot \underline{b} \quad (6)$$

where we neglect temperature variation in the perpendicular direction (over the cloud dimensions) and assume an electrostatic field.

If one now substitutes Eq. (6) in Eq. (3), and divides all terms by D_e , one obtains a complicated expression which, however, takes on a simple form in the limit $(\Omega \tau)_e \rightarrow \infty$. In this limit, Eq. (3) becomes

$$\nabla_{||} \left[\nabla_{||} n_e + \frac{e}{T_e} n_e E_{||} \right] = 0 \quad (7)$$

We assume that moving along a field line passing through the cloud, one ultimately reaches a non-conducting region (the lower atmosphere) where all currents must vanish. Hence, we integrate Eq. (7) twice and obtain

$$\frac{T_e}{e} \ln n_e - \phi = -g(r_{\perp}) \quad (8)$$

where ϕ is the electrostatic potential and g is a function of r_{\perp} only. This result for ϕ is of course only the first term in a systematic expansion of the equations in powers of $D_{\perp}/D_{||}$. [Simon and Sleeper, 1972].

Now integrate Eq. (3) along a magnetic field passing through the cloud all the way from one non-conducting terminus to the other. By the boundary condition this becomes

$$\int \nabla_{\perp} \cdot [\underline{J}_{\perp A} + \underline{J}_{\perp B} + \underline{J}_{\perp e}] dl = 0$$

where the subscript \perp denotes the last two terms in Eq. (6) and dl is a differential length along the magnetic field direction. Let us further divide this integral into that part which lies in the cloud and that which lies in the ionosphere outside the cloud. Then we write

$$\int_{\text{cloud}} \nabla_{\perp} \cdot [\underline{J}_{\perp A} + \underline{J}_{\perp B} + \underline{J}_{\perp e}] dl + \int_{\text{iono}} \nabla_{\perp} \cdot [\underline{J}_{\perp A} + \underline{J}_{\perp B} + \underline{J}_{\perp e}] dl = 0 \quad (9)$$

To lowest order in D_+/D_e , the species expression for $\nabla_{\perp} \cdot \underline{J}_{\perp}$, obtained by substitution of Eq. (8) in Eq. (6), is

$$\frac{1}{e} \nabla_{\perp} \cdot \underline{J}_{\perp} = \pm \nabla_{\perp} \cdot \left(-D_{\perp} \nabla_{\perp} n \mp \mu_{\perp} n \nabla_{\perp} g \mp \frac{\mu_{\perp} T_e n}{e} \nabla_{\perp} n_e \right) \mp \mu_{\perp} (nT) \nabla_{\perp} n \times \nabla_{\perp} g \cdot \underline{b} \mp \mu_{\perp} (nT) \frac{T_e}{e n_e} \nabla_{\perp} n \times \nabla_{\perp} n_e \cdot \underline{b} \quad (10)$$

We now assume that, in the cloud portion of the integral in Eq. (9), the ambient ions are negligible compared to the barium ions. Thus,

$$\begin{aligned} n_B &= n_e \\ n_A &\cong 0 \end{aligned} \quad (\text{cloud region})$$

and that the reverse is true in the ionosphere portion,

$$\begin{aligned} n_A &= n_e \\ n_B &\cong 0 \end{aligned} \quad (\text{ionosphere region})$$

With this assumption, Eq. (9), evaluated to lowest order in D_+/D_e , takes the form:

$$\begin{aligned} \nabla_{\perp} \cdot [-D_{\perp} \nabla_{\perp} N_c - \mu_{\perp} N_c \nabla_{\perp} g] + \frac{\mu_{\perp}}{(\eta\tau)_c} \nabla_{\perp} g \times \underline{b} \cdot \nabla_{\perp} N_c \\ + \nabla_{\perp} \cdot \left[\underline{\Gamma}_{\perp D} - \frac{\Sigma_B}{e} \nabla_{\perp} g \right] + \frac{c}{B} \underline{\lambda}_{\perp H} \cdot \nabla_{\perp} g \times \underline{b} = 0 \end{aligned} \quad (11)$$

Here we have defined

$$\begin{aligned} N_c &\equiv \int_{\text{cloud}} n_B dl \\ D_{\perp} &\equiv D_{\perp}^B + \frac{\mu_{\perp}^B T_e}{e} = D_{\perp}^B \left(1 + \frac{T_e}{T_B}\right) \\ \mu_{\perp} &\equiv \mu_{\perp}^B \\ \underline{\Gamma}_{\perp D} &\equiv - \int_{\text{iono}} (D_{\perp}^A + \frac{\mu_{\perp}^A T_e}{e} - 2D_{\perp}^e) \nabla_{\perp} n_A dl \\ \Sigma_B &\equiv e \int_{\text{iono}} (\mu_{\perp}^A + \mu_{\perp}^e) n_A dl \\ \underline{\lambda}_{\perp H} &\equiv - \frac{B}{c} \int_{\text{iono}} [\mu_{\perp}^A (\eta\tau)^A - \mu_{\perp}^e (\eta\tau)^e] \nabla_{\perp} n_A dl \end{aligned} \quad (12)$$

and neglected variation of diffusion coefficients over the dimensions of the cloud. We have allowed for electron cross-field transport contributions in the lower ionosphere in the definitions of $\underline{\Gamma}$, Σ and $\underline{\lambda}$. Note that Σ_B is the height integrated (actually along a field line) Pedersen conductivity of the ionosphere.

One obtains a complete set of equations by combining Eq. (11) with the barium ion continuity equation integrated over the length of the cloud and evaluated to lowest order in D_+/D_e ,

$$\begin{aligned} \frac{\partial N_c}{\partial t} + \nabla_{\perp} \cdot [-D_{\perp} \nabla_{\perp} N_c - \mu_{\perp} N_c \nabla_{\perp} g] \\ - \mu_{\perp} (\eta\tau)_c \nabla_{\perp} g \times \underline{b} \cdot \nabla_{\perp} N_c = 0 \end{aligned} \quad (13)$$

and the continuity equation for the ambient ions. These represent a set of coupled integro-differential equations in the variables $N_c(r_\perp, t)$, $g(r_\perp, t)$ and $n_A(r, t)$. We now partially decouple these by the assumption that variations in the ambient ion density have small influence on the dynamics of the ion cloud. This, in effect, neglects the back effect of image striations [Völk and Haerendel, 1971] on the cloud. With this assumption, we set n_A in Eq. (11) equal to its value in the undisturbed ionosphere which means that $\nabla_\perp n_A = 0$, $\underline{\Gamma}_\perp D = 0$, $\underline{\lambda}_\perp H = 0$, $\nabla_\perp \Sigma_B = 0$ (all, over the dimensions of the cloud) and Σ_B itself is the height integrated Pedersen conductivity of the undisturbed ionosphere. Eq. (11) reduces to:

$$\nabla_\perp \cdot \left[-D_\perp \nabla_\perp N - \mu_\perp N \nabla_\perp g \right] + \frac{\mu_\perp}{(\Omega\tau)} \nabla_\perp g \times \underline{b} \cdot \nabla_\perp N - \frac{\Sigma_B}{e} \nabla_\perp^2 g = 0 \quad (14)$$

where we drop the subscript on N and $(\Omega\tau)$ and where this equation plus Eq. (13) comprises a complete set. The boundary conditions appropriate to an ion cloud created suddenly in a localized region at $t=0$ are

$$\begin{aligned} N &\rightarrow 0 & \text{as } r_\perp &\rightarrow \infty \\ -\nabla_\perp g &\rightarrow \underline{E}_A & \text{as } r_\perp &\rightarrow \infty \end{aligned} \quad (15)$$

where \underline{E}_A is the ambient electric field (in the neutral rest frame). Eq. (14) is essentially equivalent to Eq. (8) of Simon and Sleeper [1972] while Eq. (13) is the integrated form of Eq. (1) of that paper. In that paper, these equations

were solved in the limit $\Sigma_B \gg e\mu_{\perp}N$, i.e. highly conducting background ionosphere. In this paper, we describe a new numerical technique which allows us to solve the equations for arbitrary values of Σ_B .

DYNAMICAL EQUATIONS FOR EQUILIBRIUM AND PERTURBATION

We shall solve Eqs. (13) and (14) in two stages (which are entwined in the actual numerical procedure). First a numerical solution for a time and space dependent cloud equilibrium with slab geometry is obtained. If we choose the B- field in the z-direction and assume that the density and electric fields vary only in the x-direction, Eq. (14) becomes:

$$\frac{\partial}{\partial x} \left[-D_{\perp} \frac{\partial N}{\partial x} - \mu_{\perp} N \frac{\partial g^{\circ}}{\partial x} \right] + \frac{\mu_{\perp}}{(\sigma\tau)} \frac{\partial g^{\circ}}{\partial y} \frac{\partial N}{\partial x} - \frac{\Sigma_B}{e} \frac{\partial^2 g^{\circ}}{\partial x^2} = 0$$

Integrating this once from the interior of the cloud to a distant point, using the boundary conditions in Eq. (15), one has

$$-\frac{\partial g^{\circ}}{\partial x} = \frac{E_{Ax}}{1+\lambda} + \frac{E_{Ay}}{(\sigma\tau)} \frac{\lambda}{1+\lambda} + \frac{eD_{\perp}}{\Sigma_B(1+\lambda)} \frac{\partial N}{\partial x} \quad (16)$$

where

$$\lambda(x,t) = \frac{e\mu_{\perp}N(x,t)}{\Sigma_B} \quad (17)$$

Note that $-\partial g^{\circ}/\partial y = E_{Ay}$ by the vanishing of $\nabla \times E$. This solution can then be substituted in Eq. (13) which becomes:

$$\begin{aligned} \frac{\partial N}{\partial t} - D_{\perp} \frac{\partial}{\partial x} \left(\alpha \frac{\partial N}{\partial x} \right) + \mu_{\perp} \left[E_{Ax} - \frac{E_{Ay}}{(\sigma\tau)} \right] \frac{\partial}{\partial x} (\alpha N) \\ + \frac{c}{B} E_{Ay} \frac{\partial N}{\partial x} = 0 \end{aligned} \quad (18)$$

where

$$\alpha(x, t) = \frac{1}{1 + \lambda(x, t)} \quad (19)$$

It is a straightforward matter to solve Eq. (18) numerically. Note that α represents the effect of end-shortening and that this varies from point to point.

Next, we linearize Eqs. (13) and (14) about the equilibrium derived above and fourier analyze in the y-direction (expiky). These equations are

$$\begin{aligned} \frac{\partial n_1}{\partial t} - \mathcal{D}_\perp \left[\frac{\partial^2 n_1}{\partial x^2} - k^2 n_1 \right] - \mu_\perp \frac{\partial}{\partial x} \left[N \frac{\partial g_1}{\partial x} + n_1 \frac{\partial g^0}{\partial x} \right] \\ - ik\mu_\perp (Nikg_1 - n_1 E_{Ay}) - ik\mu_\perp (n\tau) \left[g_1 \frac{\partial N}{\partial x} - n_1 \frac{\partial g^0}{\partial x} \right] \\ + \mu_\perp (n\tau) E_{Ay} \frac{\partial n_1}{\partial x} = 0 \end{aligned} \quad (20)$$

and

$$\begin{aligned} -\mathcal{D}_\perp \frac{\partial^2 n_1}{\partial x^2} - \mu_\perp \frac{\partial}{\partial x} \left(n_1 \frac{\partial g^0}{\partial x} \right) - \mu_\perp \frac{\partial}{\partial x} \left(N \frac{\partial g_1}{\partial x} \right) \\ + \left[\mathcal{D}_\perp k^2 + ik\mu_\perp E_{Ay} - ik \frac{\mu_\perp}{n\tau} \frac{\partial g^0}{\partial x} \right] n_1 \\ - \frac{\mu_\perp E_{Ay}}{(n\tau)} \frac{\partial n_1}{\partial x} - \frac{\Sigma_B}{e} \frac{\partial^2 g_1}{\partial x^2} \\ + \left[k^2 \mu_\perp N + ik \frac{\mu_\perp}{(n\tau)} \frac{\partial N}{\partial x} + k^2 \frac{\Sigma_B}{e} \right] g_1 = 0 \end{aligned} \quad (21)$$

We solve Eqs. (20) and (21) by studying the growth in time of some arbitrary perturbations in \underline{x} . Details of the numerical procedure are given in Appendix B.

Throughout our numerical procedure we assume that the initial density distribution is a gaussian with characteristic length h . Thus

$$N(t=0) = \bar{N} e^{-(x/h)^2} \quad (22)$$

Using this characteristic length h and the initial central density \bar{N} we define the dimensionless variables

$$\begin{aligned} x^* &= x/h, & t^* &= tD_{\perp}/h^2 \\ \lambda^* &= e\mu_{\perp}\bar{N}/\Sigma_B, & N^* &= N/\bar{N} \\ E^* &= \mu_{\perp}Eh/D_{\perp}, & k^* &= kh, & g^{\circ*} &= g^{\circ}\mu_{\perp}/D_{\perp} \\ n_i^* &= n_i/\bar{N} & \text{and} & & g_i^* &= g_i\mu_{\perp}/D_{\perp} \end{aligned}$$

and transform to the frame moving with the velocity $\frac{cF_{Ay}}{B}$. The dimensionless form of Eqs. (18) - (21) are

$$\frac{\partial N}{\partial t} - \frac{\partial}{\partial x} \left(\alpha \frac{\partial N}{\partial x} \right) + \left[E_{Ax} - \frac{E_{Ay}}{(\Omega\tau)} \right] \frac{\partial}{\partial x} (\alpha N) = 0 \quad (23)$$

$$\alpha = \frac{1}{1 + \lambda N} \quad (24)$$

$$\begin{aligned} \frac{\partial n_i}{\partial t} - \frac{\partial^2 n_i}{\partial x^2} - \frac{E_{Ay}}{(\Omega\tau)} \frac{\partial n_i}{\partial x} - \frac{\partial}{\partial x} \left(\frac{\partial g^{\circ}}{\partial x} n_i \right) \\ + \left(k^2 + ikE_{Ay} + ik\Omega\tau \frac{\partial g^{\circ}}{\partial x} \right) n_i \\ - \frac{\partial}{\partial x} \left(N \frac{\partial g_i}{\partial x} \right) + \left[k^2 N - ik(\Omega\tau) \frac{\partial N}{\partial x} \right] g_i = 0 \end{aligned} \quad (25)$$

$$\begin{aligned}
 & -\frac{\partial^2 n_1}{\partial x^2} - \frac{E_{Ay}}{(\Omega\tau)} \frac{\partial n_1}{\partial x} - \frac{\partial}{\partial x} \left(\frac{\partial g^0}{\partial x} n_1 \right) + [k^2 + ikE_{Ay} \\
 & - \frac{ik}{(\Omega\tau)} \frac{\partial g^0}{\partial x}] n_1 - \frac{1}{\lambda} \frac{\partial^2 g_1}{\partial x^2} - \frac{\partial}{\partial x} \left(N \frac{\partial g_1}{\partial x} \right) \\
 & + [k^2(N + \frac{1}{\lambda}) + \frac{ik}{(\Omega\tau)} \frac{\partial N}{\partial x}] g_1 = 0
 \end{aligned} \tag{26}$$

where all quantities are in dimensionless units and we have suppressed the asterisk. Also

$$-\frac{\partial g^0}{\partial x} = \frac{E_{Ax}}{1+\lambda N} + \frac{\lambda}{1+\lambda N} \frac{\partial N}{\partial x} + \frac{E_{Ay}}{(\Omega\tau)} \frac{\lambda N}{1+\lambda N} \tag{27}$$

in the same units. In practice, we work with Eq. (26) and the difference of Eqs. (25) and (26), which is

$$\begin{aligned}
 & \frac{\partial n_1}{\partial t} + ik \frac{\partial g^0}{\partial x} \frac{[1+(\Omega\tau)^2]}{(\Omega\tau)} n_1 + \frac{1}{\lambda} \left(\frac{\partial^2 g_1}{\partial x^2} - k^2 g_1 \right) \\
 & - ik \frac{[1+(\Omega\tau)^2]}{(\Omega\tau)} \frac{\partial N}{\partial x} g_1 = 0
 \end{aligned} \tag{28}$$

Note that the entire behavior of a given k perturbation depends only on λ , E_{Ax} , E_{Ay} , and $\Omega\tau$ for the barium ions. It is also worth noting that the equilibrium electric field in the cloud interior (in dimensionless units) follows from Eq. (8) and is

$$E_x = -\frac{\partial g^0}{\partial x} - \frac{T_e/T_B}{1+(T_e/T_B)} \frac{1}{N} \frac{\partial N}{\partial x}$$

$$E_y = E_{Ay}$$

Note also that the boundary conditions on n_1 and g_1 are that $n_1 \rightarrow 0$ and $\nabla g_1 \rightarrow 0$ as $|x| \rightarrow \infty$.

NUMERICAL SOLUTIONS AND DISCUSSION

Solutions are obtained by integrating forward in time using an initial gaussian for the equilibrium and an initial density perturbation consisting of a sum of several Hermite polynomials with amplitudes appropriate to white-noise and with randomly selected phases. A linear instability is detected by observing the growth in time of the average density disturbance defined as:

$$\langle n_{1k} \rangle = \left[\frac{\int_{-\infty}^{\infty} |n_{1k}(x,t)|^2 dx}{\int_{-\infty}^{\infty} |n_{1k}(x,0)|^2 dx} \right]^{1/2} \quad (29)$$

Details of the computational procedure are given in Appendix B. Let us now examine a number of the results.

Variation with λ . To study the effect of variations in λ , we fixed the remaining variables at $(\Omega\tau)=10$, $E_x=1$, $E_y=-10$. The magnitudes of $(\Omega\tau)$ and $|E|$ are roughly in the range of experimental releases while the E_x, E_y ratio is arbitrary. Some typical time developments of the equilibrium solution are shown in Fig. 1 for three values of λ ; 0.25, 4 and 50 corresponding to strong shorting, a typical experimental value and weak shorting, respectively. Note that in the strong shorting case, there is diffusion at the ion perpendicular rate as expected [Simon, 1955] and that very little distortion occurs since the shorting ratio α remains close to unity at all times. The drift to the right is due to the combined effect of Pedersen ion current and the actual E_{Ay} drift being $(\Omega\tau)^2 cE_{Ay}/B[1+(\Omega\tau)^2]$ rather than cE_{Ay}/B . In the more typical second case, we see reduced diffusion and distortion of the cloud

due to the varying value of α across the cloud. Finally, in the weak shorting case, we see a cloud controlled almost entirely by electrons (ambipolar cross-field diffusion). Since we assumed $(\Omega\tau)_e \rightarrow \infty$, there is little change in time.

The time behavior of some perturbations about the $\lambda=4$ equilibrium are shown in Fig. 2. Note that the growing modes rapidly approach an exponential growth and that there is a fastest growing mode in the vicinity of $k=4$. Very short and very long wavelengths are stable. In fact, in a much longer timescale, the growth rates of all the growing modes decrease and some become stable as the equilibrium diffuses and its density gradient decreases. It is interesting to note that the growing modes are localized on the rear of the cloud as may be seen from the spatial evolution of the $k=4$ mode as shown in Fig. 3.

Some idea of the effect of variation in λ upon these results is seen from the plot in Fig. 4 of the exponential growth rate γ_k ,

$$\gamma_k = \langle n_{iR} \rangle^{-1} \frac{d\langle n_{iR} \rangle}{dt} \quad (30)$$

versus k from various values of λ (γ_k evaluated at $t=0.02$). Note the strong dependence on λ . For no end-shortening $\lambda=\infty$, all values of k are unstable and γ approaches an asymptotic value as $k^2 \rightarrow \infty$. This is in qualitative agreement with the results in Linson and Workman [1970] and indeed with the result in Simon [1963] if one takes the limit $(\Omega\tau)_e \rightarrow \infty$ in that paper. As λ decreases, the growth rate decreases and a finite range of unstable k is established. For strong shorting all

modes are stable for λ slightly less than 0.5.

It is interesting to compare the magnitude of the growth rate with the simple estimate [Linson and Workman, 1970]

$$\gamma \cong \frac{c E_0}{B h} \quad (31)$$

In dimensionless units, this is

$$\gamma^* = \frac{1 + (n\tau)^2}{(n\tau)} E_0^* \cong 100 \quad (32)$$

in our case. We see, from Fig. 4, that the growth is about seven times this value for $\lambda = \infty$ and rapidly decreases as λ decreases.

Variation with $|E_A|$. Next we fix the angle between E_A and the slab normal at $E_{Ay}/E_{Ax} = -10$, set $\lambda = 4$ and vary $|E_A|$. The resulting growth rates (at $t=0.2$) are shown in Fig. 5. Note the rapid decrease in both maximum growth and range of unstable k as $|E_A|$ decreases. In fact, if one plots γ_{MAX} versus E_y , as shown in Fig. 6, one obtains a straight line which crosses the axis at about $E_y^* = -0.5$ for $\lambda = y$. Note that as λ decreases, the critical value of $|E_A|$ increases. The linear dependence indicates that γ_{MAX} does indeed vary directly as $c E_A / B h$. Indeed in this range of λ , γ_{MAX} varies roughly as

$$\gamma_{MAX} = \frac{a \lambda}{b + \lambda} E_A - \frac{c}{\lambda^d} \quad (33)$$

where a , b , c and d are constants.

Variation with Electric Field Angle. If we define $\theta \equiv \tan^{-1}(E_y/E_x)$, the variation of γ (at $t=0.2$) with θ is shown in Fig. 7. The growth rate is largest at angles close to $\pi/2$ and $-\pi/2$ [the $-\pi/2$ curve is identical to that for

$+\pi/2$]. It is somewhat higher for the positive values. All modes are stable at $\theta=0$. This is not a general result. Instability occurs at $\theta=0$ for large values of $|E_A|$ for small $(\Omega\tau)$. A plot of the angular variation for two other values of $|E_A|$ is shown in Fig. 8.

Variation with $(\Omega\tau)$. The variation of γ with $\Omega\tau$ is shown in Fig. 9. One should remember however that the dimensionless growth rate includes $(\Omega\tau)$ in its definition. In real time

$$\begin{aligned} \gamma_{MAX} &= \gamma_{MAX}^* \frac{c(T_i + T_e)}{e B h^2} \frac{(\Omega\tau)}{1 + (\Omega\tau)^2} \\ &= \gamma_{MAX}^* \frac{1}{E_A^*} \frac{c E_A}{B h} \frac{(\Omega\tau)}{1 + (\Omega\tau)^2} \end{aligned} \quad (34)$$

Hence, we plot $\gamma_{MAX}^*(\Omega\tau)/[1+(\Omega\tau)^2]$ versus $(\Omega\tau)$ and observe that the real growth rate increases with increasing $(\Omega\tau)$ and approaches a constant value for large $(\Omega\tau)$. This is shown in Fig. 10. Note that this is close to the value $c E_A/Bh$ (for $\lambda=4$).

Shape of Fastest Mode. We note that the maximum value of k for values of λ in the neighborhood of $\lambda=4$ are of the order of $k=4$. This corresponds to a true wavelength in the y direction which is $\lambda_y = 2\pi h/k^* \cong \frac{\pi}{2} h$. Thus, the fastest growing mode will have comparable dimensions in both the x and y - directions. A plot of the density perturbation is given in Fig. 11. The corresponding perturbation in g_1 is shown in Fig. 12. Note that the g_1 maxima are displaced a quarter-wavelength from the density maxima.

Discussion. In summary, we have demonstrated that one must include finite ionospheric end-shortening of the cloud

in order to obtain a most favored growth mode of reasonable size and that the results are quite sensitive to the shorting ratio. Previous results can be explained in terms of either no end shorting or no diffusion (all k unstable) or large end-shortening (all k stable). Shorter wavelengths are stabilized by ion diffusion at moderate values of λ . We demonstrate that the growth rate is also a sensitive function of electric field strength and angle and that the plasma is stable if $|E|$ drops below a critical value. In addition, the growth rate increases with increasing $\Omega\tau$ but becomes a constant for large values of same. The fastest growing mode, for moderate values of λ has a k about 4 corresponding to fairly circular striations in the plane perpendicular to B , and grows with a rate of the order of $c|E_A|/B h$.

One could relate this to delay time by estimating the number of e-folding times required for a thermal fluctuation to grow and appreciably modulate the original cloud. By elementary statistical mechanics, the r.m.s. fluctuation of the number of ions contained in a striation of length l and transverse dimensions h is

$$\Delta N \cong [n L h^2]^{1/2}$$

where n is the average ion number density in the cloud. Taking, as crude estimates, $n \cong 10^6 \text{ cm}^{-3}$, $h = 1 \text{ km}$, $l = 10 \text{ km}$, one finds $\Delta N/N = 10^{-11} \cong e^{-25}$. If we thus assume that 25 e-folding times are required for a fluctuation of the fastest growing k -mode to reach observable size, we obtain an estimate of the delay time (in dimensionless units) as,

$$t_D^* \cong \frac{25}{\gamma_{MAX}^*} \quad (35)$$

Using the value of $\gamma_{MAX}^* \cong 60$ for $|E_A| \cong 10$ and $\lambda=4$, one would estimate a delay time of 1/2 in dimensionless units or about half the time to diffuse across the original cloud size since t in real time is $t_D = \frac{1}{2}h^2/D_{\perp}$. This is of the order of tens of minutes in many experiments.

In conclusion, we note that a two-dimensional calculation would differ from the one-dimensional one in one important way. The finite ends of the cloud in the y -direction would then allow polarization charges to accumulate and one would have a mechanism for shielding E_{AV} in the interior with consequent steepening of the cloud rear. This would add an additional steepening mechanism which should also be strongly λ -dependent. One might expect the time scale for this steepening to be at least as fast as the cross-field diffusion, so that striation and steepening would be strongly entwined. In fact, if the steepening was rapid compared to diffusion spreading, one would have a mechanism which enhanced the instability growth rate as time went on and a timeplot such as that given in Fig. 2 might well show the curves bending upwards instead of down. Further insight awaits the results of 2-D calculations which are now under study.

Appendix A

Special Cases Yielding Previous Results

No End Shorting. We show here that one recovers the results of Linson and Workman [1970] in the limit where $\Sigma_R \rightarrow 0$. This limit corresponds to $\lambda \rightarrow \infty$ and thus Eq. (23) reduces to $\partial N / \partial t = 0$ with the general solution

$$N = N(x) \quad (\text{A.1})$$

The corresponding value of ρ^0 may be obtained from Eq. (27).

In this limit

$$-\frac{\partial \rho^0}{\partial x} = \frac{1}{N} \frac{dN}{dx} + \frac{E_{Ay}}{\Omega \tau} \quad (\text{A.2})$$

We make correspondence with Linson and Workman by the choice

$$N(x) = e^{-x} \quad (\text{A.3})$$

Then

$$\frac{\partial \rho^0}{\partial x} = 1 - \frac{E_{Ay}}{\Omega \tau} = \text{constant} \quad (\text{A.4})$$

and Eq. (26) becomes:

$$\begin{aligned} -\frac{\partial^2 n_1}{\partial x^2} - \frac{\partial n_1}{\partial x} + \left[k^2 - \frac{ik}{\Omega \tau} \left(1 - \frac{E_{Ay}}{\Omega \tau} [1 + (\Omega \tau)^2] \right) \right] n_1 \\ - \frac{\partial^2}{\partial x^2} (N g_1) - \frac{\partial}{\partial x} (N g_1) + \left(k^2 - \frac{ik}{\Omega \tau} \right) N g_1 = 0 \end{aligned} \quad (\text{A.5})$$

while Eq. (28) becomes

$$\frac{\partial n_1}{\partial t} + ik \frac{[1 + (\Omega \tau)^2]}{\Omega \tau} \left(1 - \frac{E_{Ay}}{\Omega \tau} \right) n_1 + ik \frac{[1 + (\Omega \tau)^2]}{\Omega \tau} N g_1 = 0 \quad (\text{A.6})$$

Since these are linear equations in n_1 and Ng_1 , with constant coefficients, we Fourier analyze each of these variables as $\exp[i\omega t + imx]$ and immediately obtain a dispersion relation. The result is

$$\omega = - \frac{k E_{Ay} [1 + (\Omega\tau)^2]}{(\Omega\tau)} \frac{[k(\Omega\tau) - m - i(m^2 + k^2)]}{[k + m(\Omega\tau) + i(m^2 + k^2)(\Omega\tau)]} \quad (\text{A.7})$$

which one easily recognizes as precisely the dispersion relation in Linson and Workman [1970, Eq. (15)] correcting for the fact that the above result is in the frame moving with the cE_{Ay}/B velocity and is in dimensionless units. Thus, the results of Linson and Workman are for the case of no shorting by the ambient ionosphere which implies electron (ambipolar) diffusion across the magnetic field (in their actual calculation $(\Omega\tau)_e \rightarrow \infty$) and strong instability since the stabilizing effect of end-shortening is removed. It should be noted that finite electron diffusion [$(\Omega\tau)_e$ finite rather than infinite] does stabilize very short wavelengths, but this is for lengths very much shorter than those stabilized by ion diffusion (by the ratio $[(\Omega\tau)_+ / (\Omega\tau)_e]^{1/2}$) and much smaller than striation lengths seen in actual experiments.

Infinite End Shortening. In this case $\Sigma_R \rightarrow \infty$ and $\lambda \rightarrow 0$.

From Eq. (26), we see that in this limit

$$\frac{\partial^2 g_1}{\partial x^2} - k^2 g_1 = 0 \quad (\text{A.8})$$

The only solution that vanishes at $x = \pm\infty$ is

$$g_1 = 0 \quad (\text{A.9})$$

By the equilibrium condition in Eq. (27), we have

$$\frac{\partial \varphi^0}{\partial x} = -E_{Ax} = \text{constant} \quad (\text{A.10})$$

Hence Eq. (25) becomes:

$$\begin{aligned} \frac{\partial n_1}{\partial t} - \frac{\partial^2 n_1}{\partial x^2} + (E_{Ax} - \frac{E_{Ay}}{\eta\tau}) \frac{\partial n_1}{\partial x} \\ + [k^2 - ik(\eta\tau)(E_{Ax} - \frac{E_{Ay}}{\eta\tau})] n_1 = 0 \end{aligned} \quad (\text{A.11})$$

which obviously has decaying solutions only. Hence, all perturbations are stable in the case of infinite end-shorting (and in the limit $n_+/n_e = 0$, as was assumed in the derivation of the basic equations).

Ion Diffusion Neglected. We recover the results of Völk and Haerendel [1971] if we use the approximations in their paper. These are (in our notation),

$$\begin{aligned} N &= N_0 \exp(-Kx) \\ E_{Ax} &= 0 \end{aligned} \quad (\text{A.12})$$

$$k_x = 0, \quad \text{i.e.} \quad \frac{dn_1}{dx} = \frac{d\varphi_1}{dx} = 0$$

and neglect of $D_{\perp} \nabla n$ compared to $\mu_{\perp} n \underline{E}$. This last assumption, in dimensionless notation, means

$$E_{Ay} \gg 1 \quad (\text{A.13})$$

We now apply these to Eq. (25) and obtain

$$ikE_{Ay} n_1 + k^2 (N + \frac{1}{\lambda}) \varphi_1 = 0 \quad (\text{A.14})$$

where we take $(\Omega\tau) \gg 1$ and use Eq. (27) to see that $\partial g^0/\partial x$ has two terms of order unity and $E_{Ay}/\Omega\tau$, respectively. Now using this result and our approximations in Eq. (28) we obtain

$$\frac{\partial n_1}{\partial t} + \left[ik \frac{\partial g^0}{\partial x} (\Omega\tau) + \frac{ik E_{Ay}}{\lambda(1+\lambda N)} - \frac{[1+(\Omega\tau)']}{(\Omega\tau)} \frac{\partial N}{\partial x} \frac{E_{Ay}}{(N+\frac{1}{\lambda})} \right] n_1 = 0 \quad (\text{A.15})$$

The growth rate is determined by the last term only. Using the definition of the equilibrium, we find the growth rate γ to be:

$$\gamma = - \frac{[1+(\Omega\tau)']}{(\Omega\tau)} \frac{E_{Ay} K}{[1 + \frac{1}{\lambda N}]} \quad (\text{A.16})$$

This is in dimensionless units. In real units, this becomes

$$\gamma = - \frac{C}{B} E_{Ay} K \cdot \left(1 + \frac{\Sigma_B}{e \mu_{\perp}^c N_c} \right)^{-1} \quad (\text{A.17})$$

Comparing this with Eq. (49) of Völk and Haerendel, we see that a similar result obtains with $\Sigma_B/e \mu_{\perp}^c N_c$ playing the role of their DR. This identification is exact in the limit of small k_y .

Thus, we see that the results in Völk and Haerendel do include the effects of end shorting. However, their neglect of ion diffusion removes this stabilizing effect on short wavelengths and allows all these modes to grow at the same rate.

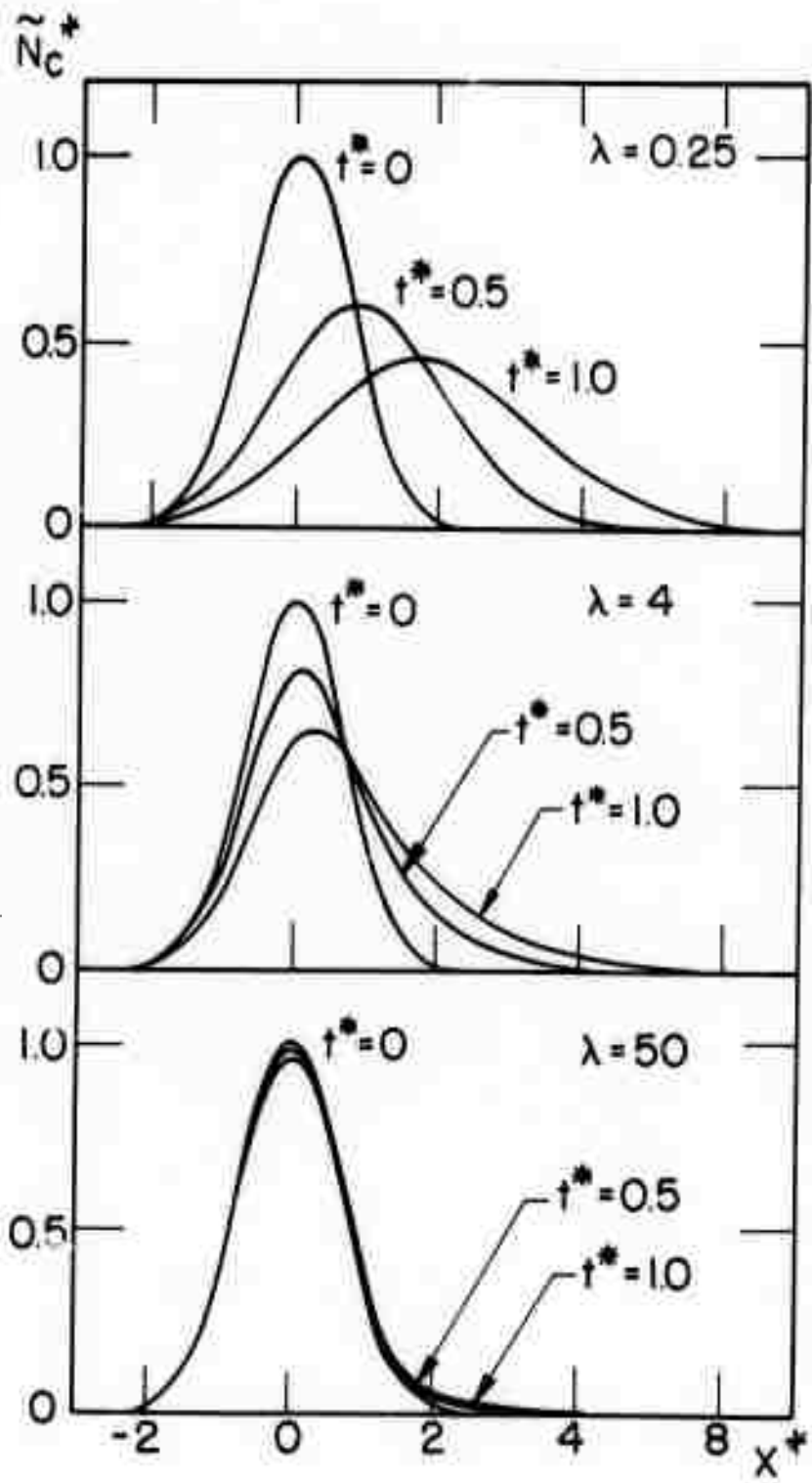
Appendix B:
Computational Procedure

Finite difference methods are used in obtaining the evolution of the equilibrium density N and the perturbations n_1 and g_1 . Equation (23) is a nonlinear parabolic equation for the unknown N . It can be solved by the Crank-Nicolson finite difference scheme with forward projection of the nonlinear coefficient [von Rosenberg, 1969]. The Crank-Nicolson analogs of (26) and (28) also provide two tridiagonal systems for the unknowns n_1 and g_1 . The grid points for evaluating n_1 and g_1 are located at time levels $t=n\Delta t$. The grid points for evaluating N are located at time levels $t=(n+\frac{1}{2})\Delta t$, so that the value of N together with $\partial g^0/\partial x$ from (27) can be easily used in evaluating the coefficient of the two tridiagonal systems.

In carrying out the computations, we first solve for the self-consistent g_1 from the initial value n_1 . We then solve for N at $t=\frac{1}{2}\Delta t$ from its initial value. The two tridiagonal systems are then solved to obtain values of n_1 and g_1 at $t=\Delta t$. We then update the value of N to $t=\frac{3}{2}\Delta t$ and solve for n_1 and g_1 at $t=2\Delta t$ and repeat these procedures. The accuracy of the results was checked by comparing results obtained using different grid spacings in space and in time and using different total number of spatial grid points with the same spacing.

REFERENCES

- Linson, L. M. and J. B. Workman, Formation of striations in ionospheric plasma clouds, *J. Geophys. Res.* 75, 3211, 1970.
- Simon, A., Ambipolar diffusion in a magnetic field, *Phys. Rev.* 98, 317, 1955.
- Simon, A., Instability of a partially ionized plasma in crossed electric and magnetic fields, *Phys. Fluids* 6, 382, 1963.
- Simon, A., Growth and stability of artificial ion clouds in the ionosphere, *J. Geophys. Res.* 75, 6287, 1970.
- Simon, A. and A. M. Sleeper, Barium cloud growth in a highly conducting medium, *J. Geophys. Res.* 77, 2353, 1972.
- Völk, H. J. and G. Haerendel, Striations in ionospheric ion clouds, 1, *J. Geophys. Res.* 76, 4541, 1971.
- Von Rosenberg, D., Methods for the numerical solution of partial differential equations, American Elsevier Publishing Co., 1969.



$\langle n_{1k} \rangle$

